Characterization of Degenerative Mitral Valve Disease Using Morphologic Analysis of Real-Time 3D Echocardiographic Images

S Chandra[1], IS Salgo[2], L Sugeng[1], L Weinert[1], M Takeuchi[3], W Tsang[1], RM Lang[1], V Mor-Avi[1]

[1]University of Chicago, Chicago, Illinois
[2]Philips Healthcare, Andover, Massachusetts, USA
[3]University of Occupational and Environmental Health, Kitakyushu, Japan

Abstract

Pre-surgical planning of mitral valve (MV) repair in patients with Barlow's disease (BD) and fibroelastic deficiency (FED) is challenging due to inability to accurately assess the complexity of MV prolapse. We hypothesized that the etiology of degenerative MV disease (DMVD) could be objectively and accurately determined using morphologic analysis of MV geometry from real-time 3D echocardiographic (RT3DE) images. Seventy-seven patients underwent transesophageal RT3DE study: 57 patients with DMVD studied intra-operatively (28 BD, 29 FED classified during surgery) and 20 patients with normal MV who were used as controls (NL). Parameters of annular dimensions and geometry, and leaflet surface area were measured. Morphologic analysis in the DMVD group revealed a progressive increase in multiple parameters from NL to FED to BD, allowing for accurate diagnosis of these entities. Strongest predictors of the presence of DMVD included billowing height and volume. 3D billowing height with a cutoff value of 1.0 mm differentiated DMVD from NL without overlap, and billowing volume with a cutoff value 1.15 ml differentiated between FED and BD without overlap. Morphologic analysis as a form of decision support of assessing MV billowing revealed significant quantifiable differences between NL, FED and Barlow, allowing accurate classification of the etiology of MV prolapse and determination of the anticipated complexity of repair. .

1. Introduction

Mitral regurgitation represents a pathophysiological spectrum of functional and structural defects of the mitral valve (MV) apparatus. Specifically, degenerative mitral valve disease (DMVD) frequently includes different degrees of annular dilation, leaflet redundancy, and chordal dysfunction, which result in variable cardiovascular morbidity and mortality. DMVD encompasses two broad categories, fibroelastic deficiency (FED) and Barlow's disease (BD) [1]. Accurate diagnosis of these entities along with their specific location and complexity is important because they require different surgical planning, which necessitates careful matching between the complexity of reparability with surgical expertise [2-4]. Differential diagnosis in DMVD is challenging because it relies on qualitative evaluation that requires a high level of clinical echocardiographic expertise. Real-time 3D echocardiography (RT3DE) using 3D transesophageal (TEE) technology allows improved visualization of the mitral valve, particularly in DMVD [5-6]. We hypothesized that RT3DE-derived measurements of valvular anatomy could be used to characterize DMVD objectively. The goal of this study was to identify quantitative 3D TEE parameters that would accurately characterize DMVD and therefore, could be used to differentiate patients with normal, FED and BD valves, estimate the complexity of disease, and thus optimize treatment strategy.

2. Methods

2.1. Population

We studied 77 patients, including 57 consecutive patients with primary DMVD and severe mitral regurgitation (MR), defined as effective regurgitant orifice area >0.40 mm² and/or vena contracta >0.7 cm [7], and 20 control subjects randomly selected from patients undergoing TEE, who had no MV pathology. Patients with DMVD underwent intra-operative TEE, during which they were classified as either BD or FED based on standard criteria [8], rather than 2D TEE findings that were available to the surgeon, who was blinded to the 3D TEE images and the results of 3D analysis. This resulted in 28 patients with BD and 29 with FED.

2.2. Imaging

After completing the clinical portion of the study, RT3DE imaging of the MV was performed using an iE33 ultrasound system (Philips), equipped with a matrix TEE

transducer (X7-2t). Initially, gain settings were optimized using the narrow-angled acquisition mode without the need for ECG gating. Zoomed RT3DE images of the entire MV were then acquired in a single cardiac cycle at frame rates of 5 to 18 Hz.

2.3. Image analysis

The 3D analysis of MV parameters was performed using custom software (MVQ, QLAB, Philips) as follows. Initially, the end-systolic frame was identified and a long-axis view of the mitral apparatus was used to determine anterior, posterior, antero-lateral, and postero-medial annular coordinates. The annulus was then manually outlined by defining annular points (figure 1A) in multiple planes rotated around the axis perpendicular to the mitral annular plane (figure 1B). The annulus was then further segmented to identify leaflet geometry and coaptation points by manually tracing the leaflets in multiple parallel long-axis planes (figure 1C) spanning the annulus from commissure to commissure. The reconstructed MV was subsequently displayed as a color-coded 3D surface representing a topographical map of the mitral leaflets (figure 1D). The software then automatically generated measurements of key parameters of annular dimensions and geometry, leaflet surface area, including billowing volume and height. Specifically, these parameters included 2D and 3D annular area, antero-posterior (AP) and commissural (CC) diameters, 3D annular perimeter, inter-commissural to antero-posterior diameter ratio, anterior to posterior non-planar MV angle, aortic-mitral angle, posterior and anterior MV leaflet area, aggregate leaflet area, billowing height and volume of the anterior segments (A1, A2, and A3) and posterior scallops (P1, P2, P3); and aggregate billowing height and volume. This 3D image analysis took 5 to 10 minutes per dataset, depending on image quality and complexity of the lesion.

2.4. Statistical analysis

Inter-group differences were compared using paired student's t-test. Significance was indicated by a p value of <0.05. Multinomial logistic regression was performed to determine which measurements are best predictors of complexity of DMVD, specifically, which parameters are best at distinguishing normal from FED and from BD patients. A classification tree analysis using recursive partitioning was developed to distinguish normal patients from those with Barlow and FED and to indicate a preliminary indication of an optimal cutoff value for the presence of DMVD and specifically, FED vs. BD. In addition, receiver operating characteristic (ROC) analysis was performed to assess the superiority of these predictors using the area under the curve (AUC).

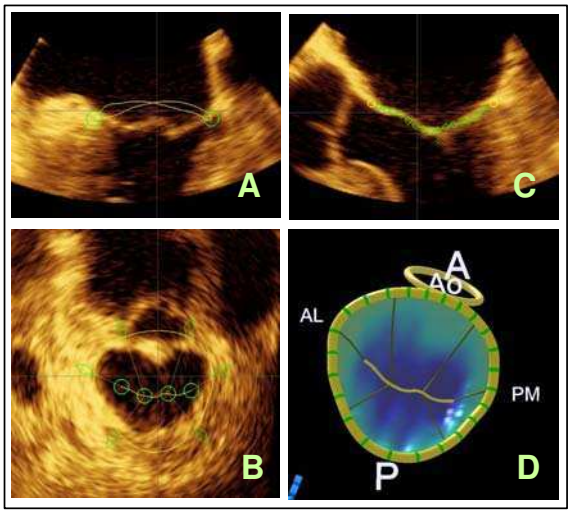

Figure 1. Morphological 3D analysis of a normal mitral valve. Mitral annulus is manually initialized in one plane (A), and then repeated in multiple rotated planes and interpolated (B); MV leaflets are manually traced from commissure to commissure in multiple parallel planes (C); the resultant surface is displayed as a color-coded 3D rendered valve surface (D).

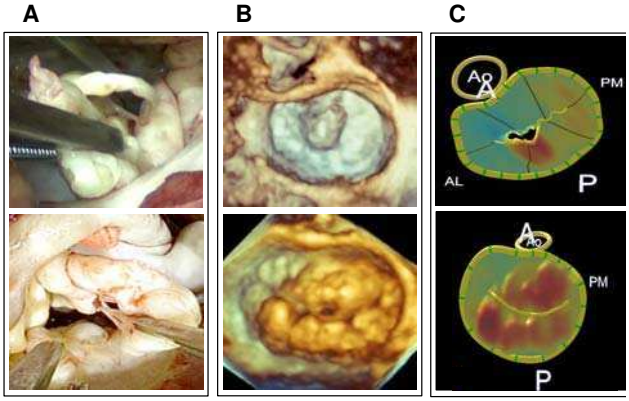

Figure 2. Examples of views of the mitral valve from the left atrial perspective obtained in two patients with degenerative mitral valve disease: (top) fibroelastic deficiency with a P2 flail leaflet and ruptured chords, and (bottom) Barlow's disease with multi-segmental billowing: (A) surgical views, (B) zoomed 3D echocardiographic views, and (C) corresponding 3D rendered color-coded images.

3. Results

Figure 2 shows surgical views, zoomed RT3DE images and their respective color-coded parametric 3D-renderings of the MV obtained in two patients with different types of DMVD. While data obtained in the control subject showed no pathology, both DMVD patient groups showed variable degrees of involvement and, as expected, larger mitral annulus and leaflet area in conjunction with multi-segmental billowing were present

in the BD patient group. The summary of results of the 3D morphologic measurements of the annular geometry, leaflet surface area, and prolapse characteristics is shown in Table 1.

Both t-test and multinomial regression analyses showed that: (1) billowing height was the strongest discriminator between control subjects and DMVD (figure 3C). (2) Billowing volume demonstrated minimal overlap between FED and BD, serving as the strongest identifier of DMVD geometric complexity in these patients (figure 3D). As expected, multi-segmental prolapse was evident in BD patients with all segments billowing to a greater degree than in their counterparts, the FED patients. In BD patients, the P2 scallop demonstrated the greatest billowing in the posterior leaflet, followed by P1 and P3 scallops (Table 1).

Classification tree analysis using recursive partitioning demonstrated that patients with billowing volumes of <1.15 ml and with billowing heights of <1 mm were normal; in contrast, patients with a billowing volumes of <1.15 ml and prolapse heights of >1 mm had FED, while those with billowing volumes >1.15 ml had BD (figure 4). The use of these cutoff values resulted in an algorithm for objective, quantitative differential diagnosis of DMVD (figure 5).

ROC curve analysis revealed high AUC values for two parameters: (i) AUC for 3D measurements of billowing height with cutoff value of >1.0 mm was 0.98; (ii) AUC for 3D measurement of billowing volume with cutoff of >1.15 ml was 1.0.

	Controls	FED	BD
3D annular area (mm^2)	797 ± 152	1154 ± 261 *	1834 ± 432 * ŦT
2D annular area (mm^2)	769 ± 148	1122 ± 250 *	1792 ± 426 * ŦT
AP diameter (mm)	28 ± 3	34 ± 5 *	44 ± 8 * ŦT
CC diameter (mm)	33 ± 3	40 ± 4 *	45 ± 9 * ŦT
CC/AP ratio	1.21 ± 0.1	1.21 ± 0.1	1.06 ± 0.3 *
3D perimeter (mm)	103 ± 10	128 ± 17 *	158 ± 19 * ŦT
Leaflet area (mm^2)	943 ± 218	1453 ± 354 *	2302 ± 455 * ŦT
Anterior leaflet area (mm^2)	472 ± 109	722 ± 178 *	1162 ± 276 * ŦT
Posterior leaflet area (mm^2)	419 ± 102	735 ± 214 *	1175 ± 306 * ŦT
Aortic-mitral angle (°)	120 ± 10	124 ± 8	123 ± 10
Non-planar angle (°)	124 ± 11	129 ± 18	155 ± 20 * ŦT
Billowing height (mm)	0.27 ± 0.23	4.10 ± 2.37 *	8.41 ± 2.91 * ŦT
Billowing volume (ml)	0 ± 0	0.34 ± 0.34 *	4.71 ± 2.52 * ŦT
A1 billowing volume (ml)	0 ± 0	0.03 ± 0.04 *	0.51 ± 0.46 * ŦT
A2 billowing volume (ml)	0 ± 0	0.03 ± 0.07 *	0.81 ± 0.68 * ŦT
A3 billowing volume (ml)	0 ± 0	0.03 ± 0.06 *	0.67 ± 0.52 * ŦT
P1 billowing volume (ml)	0 ± 0	0.05 ± 0.11 *	0.82 ± 0.61 * ŦT
P2 billowing volume (ml)	0 ± 0	0.29 ± 0.40 *	1.42 ± 0.92 * ŦT
P3 billowing volume (ml)	0 ± 0	0.08 ± 0.10 *	0.54 ± 0.45 * ŦT

Table 1. Summary of volumetric measurements of mitral valve anatomy in patients with DMVD (29 patients with fibroelastic deficiency, or FED, and 28 patients with Barlow disease) and the 20 control subjects (* - p<0.05 vs normal controls; Ŧ - p<0.05 vs FED). AP – antero-posterior; CC – inter-commissural; A1, A2 and A3 –segments 1 through 3 of the anterior leaflet; P1, P2 and P3 –scallops 1 through 3 of the posterior leaflet.

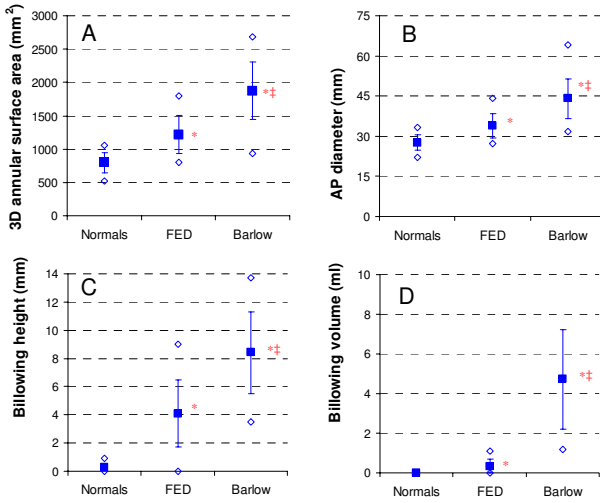

Figure 3. Graphic representation of measurements of mitral valve geometry in the 57 patients with DMVD (29 patients with fibroelastic deficiency, or FED, and 28 patients with Barlow disease) and the 20 control subjects. Solid squares with error bars represent the mean ± SD; diamonds represent the maximal and minimal values; *p<0.05 vs. normal; ‡ p<0.05 vs. FED; AP – antero-posterior.

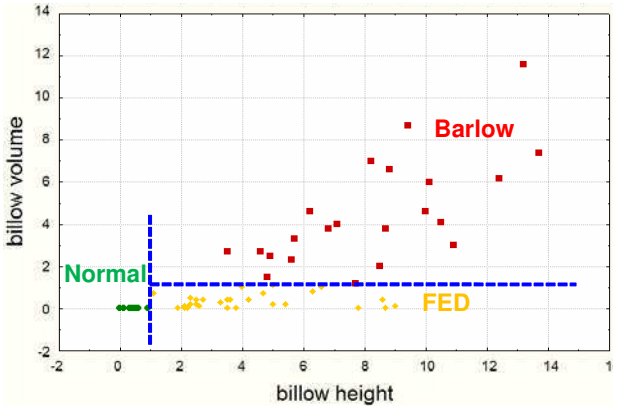

Figure 4. Scatter plots demonstrating the cutoff values of 1.0 mm for billowing height (vertical dashed line) and cutoff value of 1.15 ml for billowing volume (horizontal dashed line) in differentiating patients with BD vs. FED.

4. Discussion and conclusions

Currently, surgical inspection is the gold standard for making etiologic differentiation in DMVD patients. However, the ease of reparability, which is frequently not fully appreciated until the time of surgery, is determined by complexity of MV lesions. The lack of reliable pre-operative assessment frequently leads to inadequate match between the complexity of disease and the surgical expertise which becomes obvious only in the operating room. As a result, difficulties with pre-surgical planning and decision support may lead to either unsuccessful

repair or conversion to replacement with poor outcome in patients with complex valvular disease [9]. Accordingly, we sought to and successfully demonstrated the feasibility of using RT3DE-derived volumetric measurements of valvular anatomy to objectively evaluate MV annular and leaflet distortion in patients with DMVD prior to surgery. Furthermore, we found that this morphologic analysis was able to differentiate between degenerative and normal valves and more importantly, between the two different etiologies of DMVD, namely BD and FED. This finding could support reliably pre-operative automated clinical decision-making and thus have important surgical implications.

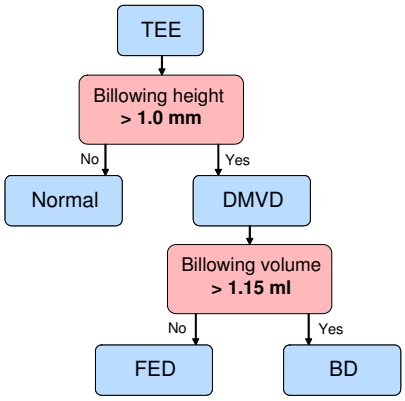

Figure 5. Clinical paradigm for use of morphologic analysis of real-time 3D echocardiographic images for differential diagnosis of degenerative mitral valve disease (DMVD) to distinguish fibroelastic deficiency (FED) from Barlow's disease (BD).

One limitation of the methodology used in this study is that the measurements are time-consuming, rely on adequate image quality and require a learning period for both imaging and data analysis. While RT3DE zoomed acquisition can be difficult to perform in patients with exceedingly large annulus, only one of the 57 DMVD patients that were screened was excluded from our study for this reason. Because surgical inspection is performed in an immobile, flaccid state, as opposed to live echocardiographic assessment, potentially resulting in discrepancy between methodologies, one might construe that using surgical findings as the gold standard reference might be a limitation of our study. However, this ability of morphologic analysis to detect small, not easily visible areas of billowing, while increasing the sensitivity of RT3DE, is likely to be diagnostically inconsequential.

In summary, our results show that 3D analysis depicts a spectrum of morphologic abnormalities that can be used to accurate differentiate degenerative from normal valves, and importantly FED from BD patients, as reflected in this study by the close agreement between 3D TEE and the surgical determinations. Moreover, this analysis facilitates not only the confirmation of etiology, but highlights quantitative anatomic differences between the groups and provides a framework for pre-operative assessment of the complexity of repair. As quantification tools become more automated and less reliant on expertise, they may be used to support clinical decision making by a wider group of physicians.

References

[1] Barlow JB, Pocock WA. Billowing, floppy, prolapsed or flail mitral valves? Am J Cardiol 55:501-502; 1985

[2] Ling LH, Enriquez-Sarano M, Seward JB, Tajik AJ, Schaff HV, Bailey KR, Frye RL. Clinical outcome of mitral regurgitation due to flail leaflet. N Engl J Med 335:1417-1423; 1996

[3] Enriquez-Sarano M, Avierinos JF, Messika-Zeitoun D, Detaint D, Capps M, Nkomo V, Scott C, Schaff HV, Tajik AJ. Quantitative determinants of the outcome of asymptomatic mitral regurgitation. N Engl J Med 352:875-883; 2005

[4] Rosenhek R, Rader F, Klaar U, Gabriel H, Krejc M, Kalbeck D, Schemper M, Maurer G, Baumgartner H. Outcome of watchful waiting in asymptomatic severe mitral regurgitation. Circulation 113:2238-2244; 2006

[5] Sugeng L, Coon P, Weinert L, Jolly N, Lammertin G, Bednarz JE, Thiele K, Lang RM. Use of real-time 3-dimensional transthoracic echocardiography in the evaluation of mitral valve disease. J Am Soc Echocardiogr 19:413-421; 2006

[6] Sugeng L, Shernan SK, Weinert L, Shook D, Raman J, Jeevanandam V, DuPont F, Fox J, Mor-Avi V, Lang RM. Real-time three-dimensional transesophageal echocardiography in valve disease: comparison with surgical findings and evaluation of prosthetic valves. J Am Soc Echocardiogr 21:1347-1354; 2008

[7] Zoghbi WA, Enriquez-Sarano M, Foster E, Grayburn PA, Kraft CD, Levine RA, Nihoyannopoulos P, Otto CM, Quinones MA, Rakowski H, Stewart WJ, Waggoner A, Weissman NJ. Recommendations for evaluation of the severity of native valvular regurgitation with two-dimensional and Doppler echocardiography. J Am Soc Echocardiogr 16:777-802; 2003

[8] Anyanwu AC, Adams DH. Etiologic classification of degenerative mitral valve disease: Barlow's disease and fibroelastic deficiency. Seminars Thorac Cardiovasc Surg 19:90-96; 2007

[9] David TE. Outcomes of mitral valve repair for mitral regurgitation due to degenerative disease. Seminars Thorac Cardiovasc Surg 19:116-120; 2007

Address for correspondence:

Victor Mor-Avi, PhD
University of Chicago MC5084,
5841 S. Maryland Ave., Chicago Illinois 60637.
E-mail: vmoravi@medicine.bsd.uchicago.edu